IOPscience iopscience.iop.org

Home Search Collections Journals About Contact us My IOPscience

The nature of intermediate-range order in Ge–As–S glasses: results from reverse Monte Carlo modeling

This article has been downloaded from IOPscience. Please scroll down to see the full text article.

2010 J. Phys.: Condens. Matter 22 115404

(http://iopscience.iop.org/0953-8984/22/11/115404)

View the table of contents for this issue, or go to the journal homepage for more

Download details:
IP Address: 129.252.86.83
The article was downloaded on 30/05/2010 at 07:35

Please note that terms and conditions apply.

IOP Publishing Journal of Physics: Condensed Matter

J. Phys.: Condens. Matter **22** (2010) 115404 (9pp) doi:10.1088/0953-8984/22/11/115404

The nature of intermediate-range order in Ge–As–S glasses: results from reverse Monte Carlo modeling

S Soyer-Uzun[1], C J Benmore[2], J E Siewenie[3] and S Sen[1]

[1] Department of Chemical Engineering and Materials Science, University of California at Davis, Davis, CA 95616, USA
[2] X-ray Science Division, Argonne National Laboratory, Argonne, IL 60439, USA
[3] Los Alamos National Laboratory, Los Alamos, NM 87545, USA

Received 10 December 2009, in final form 12 February 2010
Published 5 March 2010
Online at stacks.iop.org/JPhysCM/22/115404

Abstract

The experimental neutron and x-ray diffraction data for stoichiometric and S-deficient $Ge_xAs_xS_{100-2x}$ glasses with $x = 18.2$, 25.0, and 33.3 at.% have been modeled simultaneously using the reverse Monte Carlo (RMC) technique. Nearest-neighbor coordination environments, as obtained in previous x-ray absorption spectroscopy and diffraction experiments, have been employed as short-range order constraints in these simulations. The large scale three-dimensional structural models thus obtained from RMC simulation are used to investigate the nature and compositional evolution of intermediate-range structural order in these ternary glasses. The intermediate-range structural order is controlled by (1) a corner-shared three-dimensional network of AsS_3 pyramids and GeS_4 tetrahedra in the stoichiometric $Ge_{18.2}As_{18.2}S_{63.6}$ glass, (2) a heterogeneous structure that consists of homopolar bonded As-rich regions coexisting with a GeS_2 network in the S-deficient $Ge_{25}As_{25}S_{50}$ glass, and (3) a homogeneous structure resulting from the disruption of the topological continuity of the GeS_2 network and As-rich clusters regions due to the formation of Ge–As bonds in the most S-deficient $Ge_{33.3}As_{33.3}S_{33.3}$ glass. This scenario of the compositional evolution of intermediate-range structural order is consistent with and provides an atomistic explanation of the corresponding evolution in the position, width and intensity of the first sharp diffraction peak and the magnitude of small angle scattering in these glasses.

(Some figures in this article are in colour only in the electronic version)

1. Introduction

Chalcogenide glasses are technologically important materials that have received much attention due to their wide range of applications in active and passive photonic devices [1, 2]. The short- and intermediate-range atomic structure of simple binary chalcogenide glasses in As–X, P–X, and Ge–X (X = S, Se) systems have been studied in detail by various diffraction and spectroscopic techniques [3–15]. On the other hand, structural studies in ternary and quaternary Ge–As–S/Se/Te glasses have been mainly limited to short-range order [16–20], although a number of recent experimental studies have begun to address the nature of intermediate-range order in these systems [21–27]. Neutron and x-ray diffraction have traditionally served as the most important and direct techniques for studying intermediate-range order in amorphous materials. However, for multi-component glass systems, it is extremely difficult to extract structural information from diffraction data beyond the nearest-neighbor length scale, due to the convolution of a large number of pair-correlation functions in the radial distribution function (RDF). Systematic studies employing the observation of RDFs as a function of glass composition can be useful in terms of providing important quantitative structural information on short- and intermediate-range order. Additionally, simulation of the diffraction data using modeling techniques such as reverse Monte Carlo (RMC) modeling is often extremely useful to obtain realistic structural information in complex multi-component systems, especially at the intermediate-range length scale ($\geqslant$0.5 nm) [28, 29]. Moreover, RMC modeling of the diffraction data provides all of the partial structure factors and pair distribution functions that are important in

 © 2010 IOP Publishing Ltd Printed in the UK

Table 1. Coordination number constraints C, bond distances d and cut-off distances that are used in the RMC simulations for $Ge_xAs_xS_{100-2x}$ glasses with $x = 18.2, 25, 33.3$.

	Coordination constraints and bond distances									
Composition	C_{As-As}	d_{As-As} (Å)	C_{As-Ge} or, C_{Ge-As}	d_{As-Ge} (Å)	C_{As-S}	d_{As-S} (Å)	C_{Ge-Ge}	d_{Ge-Ge} (Å)	C_{Ge-S}	d_{Ge-S} (Å)
$Ge_{18.2}As_{18.2}S_{63.6}$	—	—	—	—	3	2.25	—	—	4	2.25
$Ge_{25}As_{25}S_{50}$	3	2.45	—	—	—	—	—	—	4	2.25
$Ge_{33.3}As_{33.3}S_{33.3}$(I)	1	2.45	2	2.45	—	—	—	—	2	2.25
$Ge_{33.3}As_{33.3}S_{33.3}$(II)	3	2.45	—	—	—	—	2	2.45	2	2.25

	Cut-off distances (Å)					
	As–As	As–Ge	As–S	Ge–Ge	Ge–S	S–S
$Ge_{18.2}As_{18.2}S_{63.6}$	3.30	3.30	2.10	3.30	2.10	3.30
$Ge_{25}As_{25}S_{50}$	2.40	3.00	3.00	3.30	2.10	3.3
$Ge_{33.3}As_{33.3}S_{33.3}$(I)	2.45	2.45	3.25	2.45	2.15	3.35
$Ge_{33.3}As_{33.3}S_{33.3}$(II)	2.30	2.30	3.25	2.30	2.10	3.25

explaining different features of the experimental diffraction results [30–39].

Here we report the RMC modeling of the structure of ternary $Ge_xAs_xS_{100-2x}$ glasses with Ge (or, As) contents of 18.2, 25, and 33.3 at.%. The nearest-neighbor coordination environments of Ge, As and S atoms in these glasses were determined using diffraction and Ge and As K-edge extended x-ray absorption fine structure (EXAFS) spectroscopic techniques, and were previously reported in the literature [16, 17, 25, 26]. These nearest-neighbor coordination constraints are used in this study to simultaneously simulate the experimental x-ray and neutron diffraction data for these glasses. The resulting structural models are used in combination with experimental diffraction data to investigate in detail the compositional evolution of the intermediate-range structural order at length scales beyond ∼0.5 nm in these glasses.

2. Experimental details

The Ge–As sulfide glasses reported in this study were synthesized by melting mixtures of the constituent elements Ge, As and S with ⩾99.995% purity (metals basis) in evacuated (10^{-6} Torr) and flame sealed fused silica ampules at ∼1200 K for at least 24 h in a rocking furnace. The ampules were quenched in water and subsequently annealed for 1 h at the respective glass transition temperatures. The neutron diffraction data that have been used in the RMC simulations were collected using the glass, liquid, and amorphous materials diffractometer (GLAD) at the intense pulsed neutron source (IPNS) at Argonne National Laboratory [40]. The x-ray diffraction experiments were carried out on the beamline 11-IDC at the Advanced Photon Source (APS) at Argonne National Laboratory. A detailed description of the experimental methods and data analysis can be found elsewhere [25, 26].

3. Reverse Monte Carlo (RMC) modeling

The RMC simulations were performed on cubic cells containing 1749, 1760, 1800 atoms for $Ge_xAs_xS_{100-2x}$ glasses with $x = 18.2$, 25 and 33.3, respectively, using the RMCA code [28, 29]. The lengths of simulation cells were determined according to the number densities of 0.0379 $Å^{-3}$, 0.0371 $Å^{-3}$ and 0.0387 $Å^{-3}$, respectively. The nearest-neighbor coordination numbers and bond distances that were used as constraints for these simulations have been obtained from the previously published diffraction and Ge and As K-edge EXAFS results for these glasses [16, 17, 25, 26], as shown in table 1. These experimental studies have shown that the Ge and As atoms have four and three nearest neighbors, respectively, irrespective of chemical composition. For the stoichiometric glass ($Ge_{18.2}As_{18.2}S_{63.6}$) the Ge and As atoms are heteropolar bonded to four and three S atoms respectively. This structure consists of a mixture of corner-shared GeS_4 tetrahedra and AsS_3 pyramids. As the metal content increases, the chemical order in the system is disrupted as heteropolar Ge/As–S bonds are gradually replaced by metal–metal bonds. At low levels of S-deficiency ($20 \leqslant x \leqslant 25$), only As atoms participate in metal–metal bonding while the GeS_4 tetrahedral units are still preserved [16, 17, 25, 26]. At the highest levels of S-deficiency ($27.5 \leqslant x \leqslant 33.3$), Ge atoms participate in metal–metal bonding after all the As atoms are used up in metal–metal bonding. However, the relative degree of chemical order in metal–metal bonding involving Ge and As atoms in this composition range can not be differentiated, even by combined neutron and x-ray diffraction. Therefore, two limiting cases were considered for RMC simulation of this composition ($x = 33.3$). Case I assumed that all Ge atoms would only bond to As atoms, and case II assumed all Ge atoms would preferentially bond to Ge atoms (table 1). All RMC models were generated following two steps. In the first step, for each glass composition, the constituent atoms are placed randomly inside the cubic cell. This initial random configuration was then modified by random atomic moves, on the basis of the nearest-neighbor bond lengths and coordination numbers listed in table 1, until each coordination constraint was met by 90–99%. Then, using these initial atomic configurations, RMC simulations were run for 10^7 steps for each composition in order to simultaneously fit the neutron and x-ray diffraction structure factors.

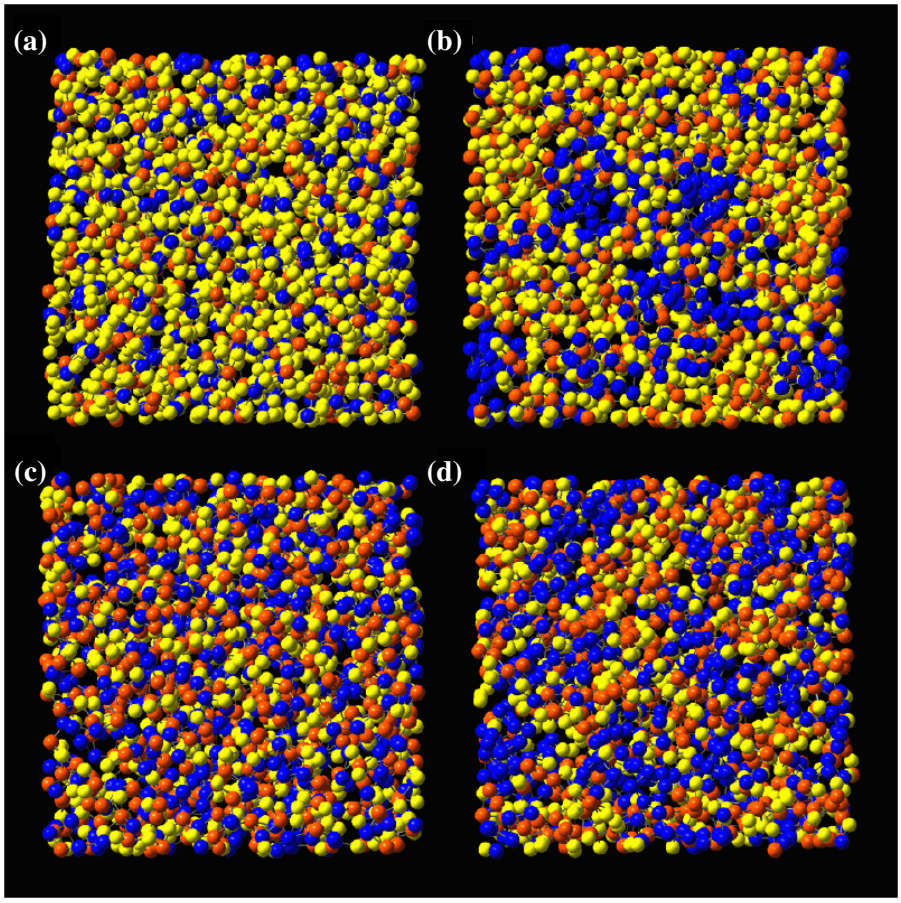

Figure 1. Atomic configurations generated by RMC simulations for $Ge_xAs_xS_{100-2x}$ glasses with Ge(or As) contents of (a) $x = 18.2$, (b) $x = 25$, (c) $x = 33.3$ for case I that assumes Ge atoms are bonded to only As atoms, and (d) $x = 33.3$ for case II that assumes Ge atoms are bonded to only Ge atoms and As atoms are bonded to only As atoms. Orange (dark gray in printed version), blue (black in printed version) and yellow (light gray in printed version) spheres represent Ge, As and S atoms, respectively.

4. Results and discussion

RMC generated three-dimensional representations of the atomic structures of the three $Ge_xAs_xS_{100-2x}$ glasses are shown in figure 1. Figures 2–5 show the experimental x-ray and neutron structure factors $S(Q)$ and the corresponding structure factors that are obtained from RMC simulations, together with the six different partial structure factors for these glasses. The experimental and RMC-simulated total neutron and x-ray structure factors show good agreement (figures 2–5). The experimental neutron RDFs $G_N(r)$ for these glasses and the partial pair distribution functions $g_{ij}(r)$ obtained from RMC simulations are compared in figures 6–9. X-ray $G(r)$s look almost the same, therefore they were not included in these figures. The respective standard definitions of $S(Q)$, $G(r)$ and $g_{ij}(r)$ can be found in previous publications [25, 26]. The peak(s) in $G(r)$, located between 2 and 3 Å, represents the nearest-neighbor coordination environments of the Ge and As atoms in the structure of these glasses. For the stoichiometric glass with $x = 18.2$ the peak centered at ∼2.2 Å corresponds to both As–S and Ge–S nearest-neighbor distances [25, 26]. A second peak at ∼2.5 Å becomes dominant in the S-deficient glasses with $x = 25$ and 33.3, and represent Ge/As–Ge/As bonds (figure 2). For the stoichiometric glass the second shell in $G(r)$ is dominated by a peak centered at ∼3.4 Å that is progressively replaced by a peak centered at ∼3.8 Å in the S-deficient glasses (figures 6–9). At distances longer than ∼4 Å the $G(r)$ has a broad peak covering the region between ∼5.0 and 5.5 Å in the stoichiometric glass, which is gradually replaced by a peak in the region between 5.5 and 6.0 Å in S-deficient glasses. Moreover, peaks at ∼7 and ∼9 Å systematically increase in intensity with decreasing S content, and become distinct, especially in the $G(r)$ of the S-deficient glasses with the lowest S contents. As discussed below, the partial pair distribution functions $g_{ij}(r)$ obtained from RMC simulations provide direct atomic assignment of these correlation peaks in the experimental $G(r)$.

4.1. Partial pair distribution functions

For $Ge_{18.2}As_{18.2}S_{63.6}$ glass, the Ge–S and As–S partial pair distribution functions display a strong peak at ∼2.25 Å corresponding to nearest-neighbor correlations. The As–As, As–Ge and Ge–Ge partial pair distribution functions show a peak at ∼3.5 Å that clearly correspond to the next-nearest neighbor environments of As and Ge atoms in Ge/As–S-Ge/As linkages. Longer-range correlations at ∼5.5 Å appear in the As–S and Ge–S partial pair distribution functions. Therefore it

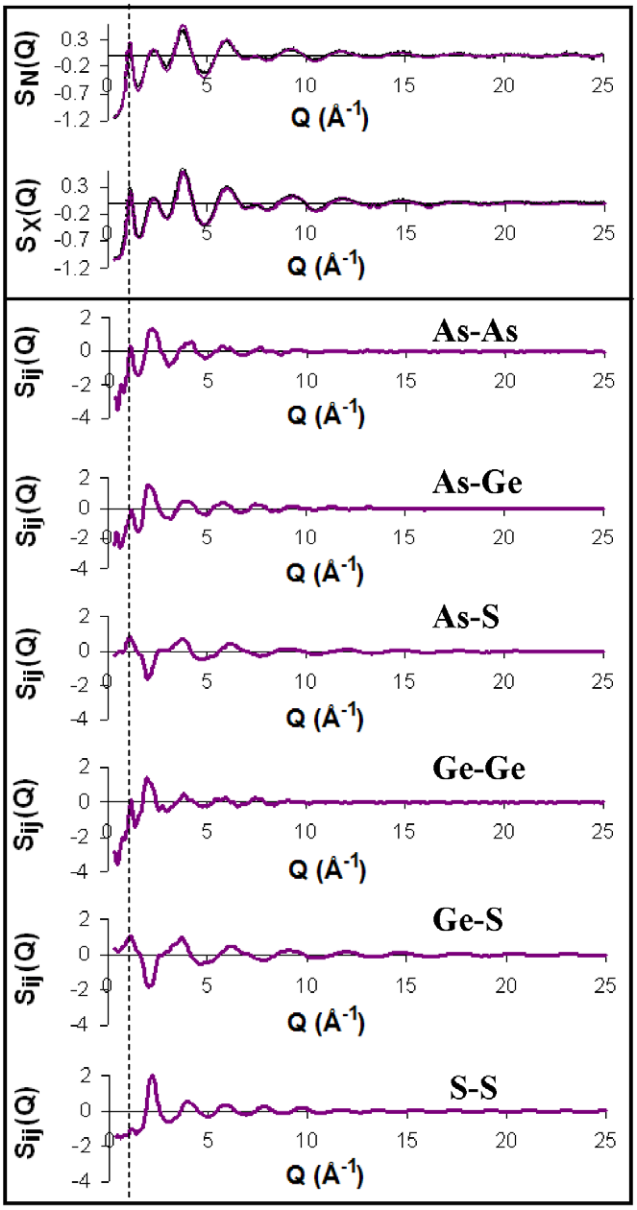

Figure 2. Upper panel: neutron and x-ray structure factors for $Ge_{18.2}As_{18.2}S_{63.6}$ glass shown in black (open circles in printed version) together with the corresponding simulated RMC fits shown in purple (solid line in printed version). Lower panel: partial structure factors $S_{ij}(Q)$ obtained from RMC simulations. The dashed line is drawn as a guide for the eye.

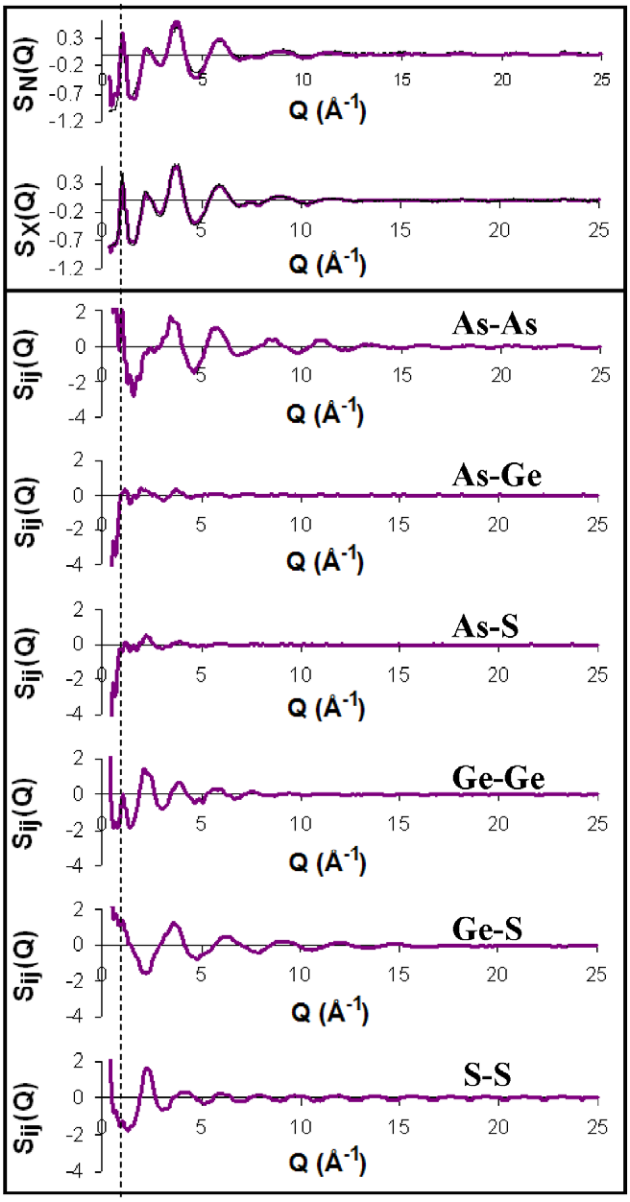

Figure 3. Upper panel: neutron and x-ray structure factors for $Ge_{25}As_{25}S_{50}$ glass shown in black (open circles in printed version) together with the corresponding simulated RMC fits shown in purple (solid line in printed version). Lower panel: partial structure factors $S_{ij}(Q)$ obtained from RMC simulations. The dashed line is drawn as a guide for the eye.

is likely that the peak located at 5.5 Å in the experimental $G(r)$ of this glass is associated with As/Ge–S correlations (figures 6–9). Moreover, the metal–metal (Ge/As–Ge/As) partial pair distribution functions display broad peaks near ∼6.5 Å. Hence, such long-range metal–metal correlations must be responsible for the broad peak in the experimental $G(r)$ covering the region between ∼6.5 and 7.0 Å.

The local coordination environment of the As atom changes in $Ge_{25}As_{25}S_{50}$ glass, as previous diffraction and Ge and As K-edge EXAFS studies have shown that all the As atoms are bonded with As atoms for this composition, while the Ge atoms still remain heteropolar bonded to S (table 1). Since these short-range order constraints were used for the RMC simulations, the resulting As–As partial pair distribution function is dominated by a sharp nearest-neighbor peak at 2.45 Å, while the Ge–S pair distribution function still exhibits a nearest-neighbor peak centered at 2.25 Å (figure 7). The peak at 3.45 Å in the Ge–Ge partial pair distribution function corresponds to Ge–Ge next-nearest neighbors that are connected through S atoms. The next-nearest neighbor peak appearing at 3.8 Å in the experimental $G(r)$ of this composition must be due to As–As next-nearest neighbors in As–As–As linkages, as the RMC-derived As–As pair distribution function exhibits a peak at ∼3.8 Å. The As–Ge correlation is very low, as there should not be many

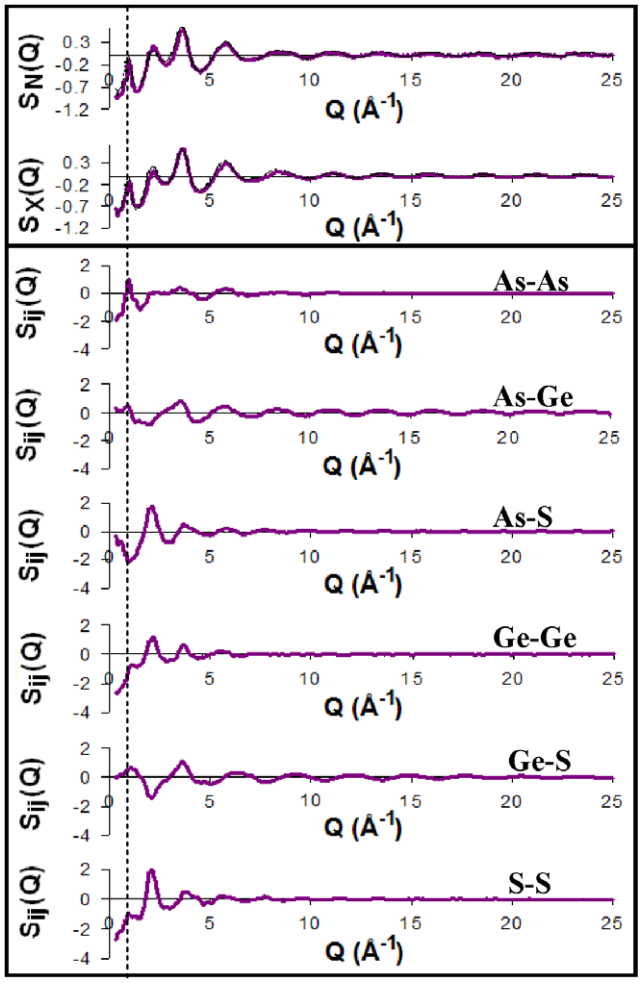

Figure 4. Upper panel: neutron and x-ray structure factors for $Ge_{33.3}As_{33.3}S_{33.3}$ glass (case I) shown in black (open circles in printed version) together with the corresponding simulated RMC fits shown in purple (solid line in printed version). Lower panel: partial structure factors $S_{ij}(Q)$ obtained from RMC simulations. The dashed line is drawn as a guide for the eye.

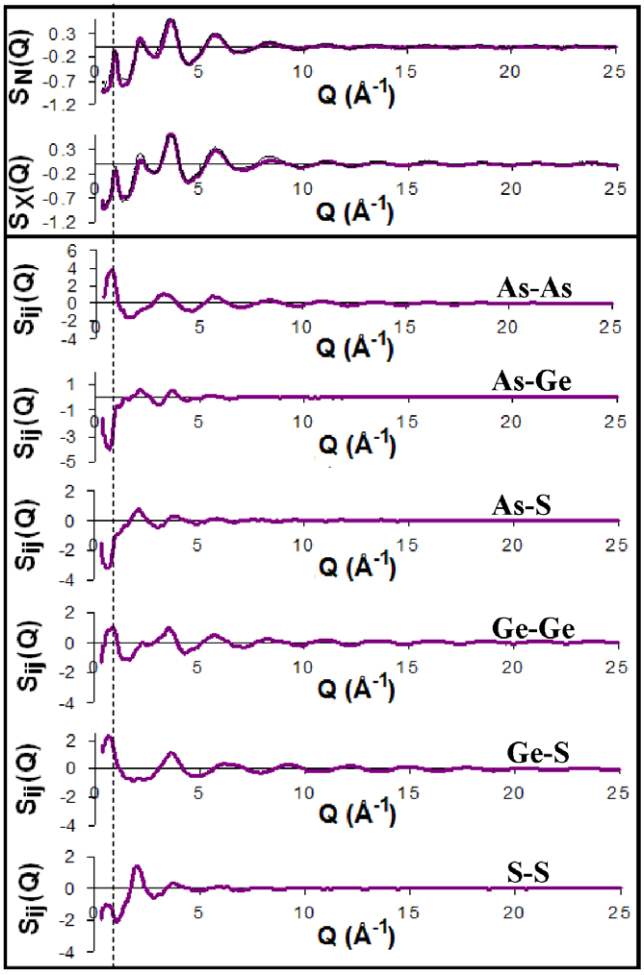

Figure 5. Upper panel: neutron and x-ray structure factors for $Ge_{33.3}As_{33.3}S_{33.3}$ glass (case II) shown in black (open circles in printed version) together with the corresponding simulated RMC fits shown in purple (solid line in printed version). Lower panel: partial structure factors $S_{ij}(Q)$ obtained from RMC simulations. The dashed line is drawn as a guide for the eye.

As–Ge next-nearest neighbors due to the extensive clustering of As atoms in homopolar bonded regions. The longer-range correlation at 5.5 Å in the experimental $G(r)$ should be related to As–As and Ge–S correlations in As-rich and GeS_2-rich clusters, respectively, as the partial pair distribution function of these correlations exhibit small peaks at ∼5.5 Å (figure 7). The broad feature at ∼6.5 Å in the Ge–Ge pair distribution function possibly indicates that the broad peak in experimental $G(r)$ is associated with Ge–Ge correlations in GeS_2 clusters.

As mentioned before, two structural scenarios were considered for the simulation of the $Ge_{33.3}As_{33.3}S_{33.3}$ glass. The corresponding partial pair distribution functions are consistent with the coordination constraints provided for each case, as expected (figures 8 and 9). Case I is possibly a more realistic structural scenario, in the sense that it would be more likely to result in a decreasing FSDP intensity and coherence length of intermediate-range order, consistent with experimental results (see discussion below). Therefore, the partial pair distribution functions for this case are discussed. For case I, where homopolar Ge–Ge bonding is excluded, the nearest-neighbor coordination environment of Ge atom is represented by the peaks at 2.25 Å and 2.45 Å in the Ge–S and As–Ge pair distribution functions, respectively (figure 8). The peaks at ∼3.8 Å in the As–As and As–Ge pair distribution functions are related to the metal–metal next-nearest neighbors that are in Ge/As–As–Ge/As linkages and are responsible for the appearance of the peak at 3.8 Å in x-ray and neutron $G(r)$s of this glass composition. Moreover, As–As and Ge–Ge correlations display broad features at ∼7 Å and As–As, As–Ge, and Ge–Ge correlations exhibit peaks at ∼5.5 Å for this composition. This observation indicates that all of the inter-atomic correlations in the experimental $G(r)$ of this glass are dominated by various metal–metal correlations, as expected from its metal-rich composition.

4.2. Structure factors

Besides deciphering the inter-atomic correlations in the experimental $G(r)$, these RMC simulations also allow for a direct understanding of the origin and nature of the first

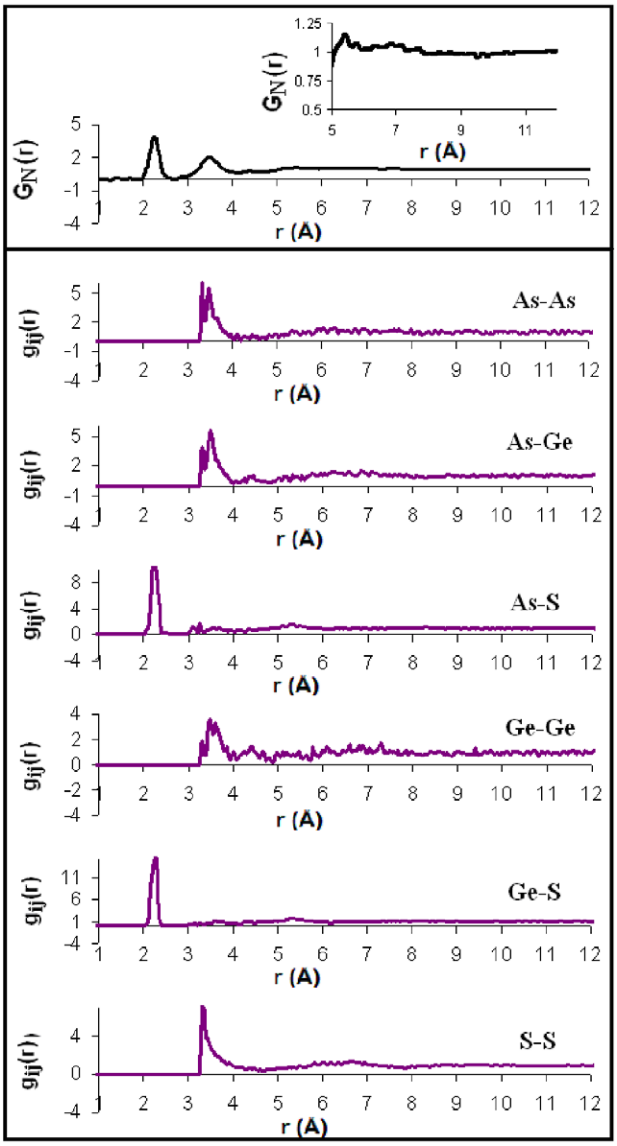

Figure 6. Upper panel: weighted average of the partial pair distribution function $G_{\mathrm{N}}(r)$ for $Ge_{18.2}As_{18.2}S_{63.6}$ glass obtained by neutron diffraction. Inset is a magnified view of $G_{\mathrm{N}}(r)$ at $r \geqslant 5$ Å. Lower panel: partial pair distribution functions $g_{ij}(r)$ for $Ge_{18.2}As_{18.2}S_{63.8}$ glass obtained from RMC simulations.

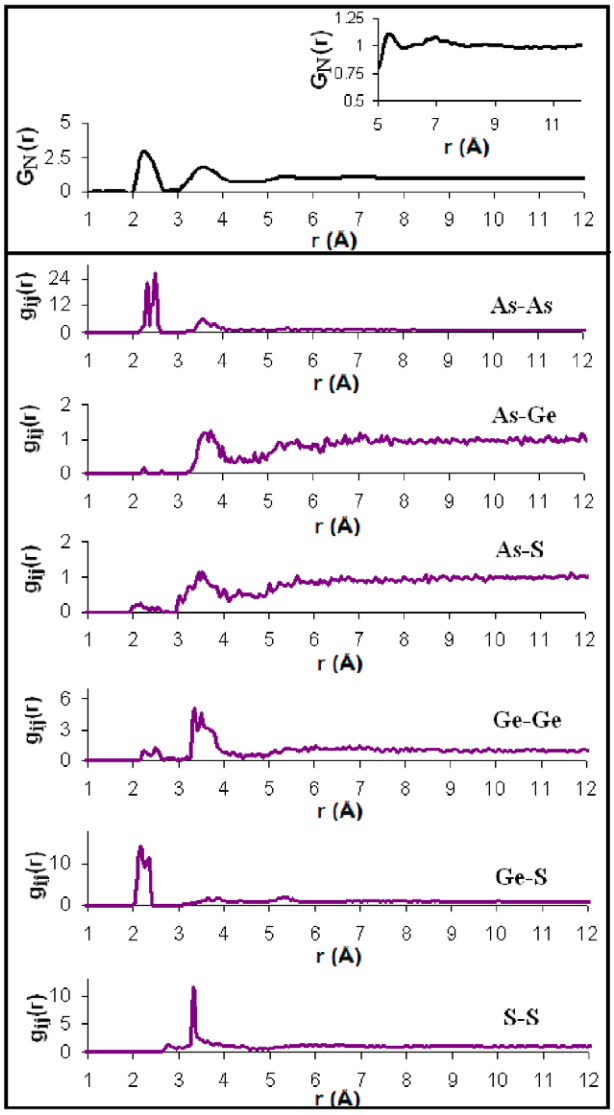

Figure 7. Upper panel: weighted average of the partial pair distribution function $G_{\mathrm{N}}(r)$ for $Ge_{25}As_{25}S_{50}$ glass obtained by neutron diffraction. Inset is a magnified view of $G_{\mathrm{N}}(r)$ at $r \geqslant 5$ Å. Lower panel: partial pair distribution functions $g_{ij}(r)$ for $Ge_{25}As_{25}S_{50}$ glass obtained from RMC simulations.

sharp diffraction peak (FSDP) and, consequently, the nature of the associated intermediate-range order in these glasses. Previous diffraction studies have shown that x-ray and neutron FSDP positions shift systematically to lower Q values with increasing metal content [25, 26]. The x-ray/neutron FSDP position is located at about 1.13 $\mathrm{Å}^{-1}$ for the stoichiometric glass composition ($x = 18.2$), while it shifts to ∼1.04 $\mathrm{Å}^{-1}$ for S-deficient glass with $x = 25$. For the glass with the highest S-deficiency ($x = 33.3$), the FSDP is located at ∼0.96 $\mathrm{Å}^{-1}$. On the other hand, the FSDP intensity was observed to increase in the composition range $18.2 \leqslant x \leqslant 25$, followed by a rapid drop in the composition range of $25 \leqslant x \leqslant 33.3$ [25, 26]. Similarly, the coherence length λ of intermediate-range order ($\lambda = 2\pi/\Delta Q_{\mathrm{FSDP}}$, where ΔQ_{FSDP} is the full width at half maximum of the FSDP) was found to be ∼18–19 Å for the stoichiometric composition, and it rapidly jumps up to about 23–24 Å for the S-deficient glass with $x = 25$, followed by a drop to ∼21 Å for the glass with $x = 33.3$. The intensity of small angle neutron scattering (SANS) that is typically associated with density and composition fluctuation also follows a similar trend, with the glass with $x = 25$ being characterized by the highest SANS intensity [25, 26]. As we discuss below, the RMC-derived structural models are completely consistent with such a composition dependence of the FSDP parameters and SANS intensity, and yield a uniquely detailed picture of intermediate-range order in the structures of these glasses.

Previous isotope-substituted neutron diffraction and anomalous x-ray scattering studies have indicated that the FSDP in chalcogenide glasses arises primarily from metal–metal correlations [12, 15, 41, 42]. The monotonically

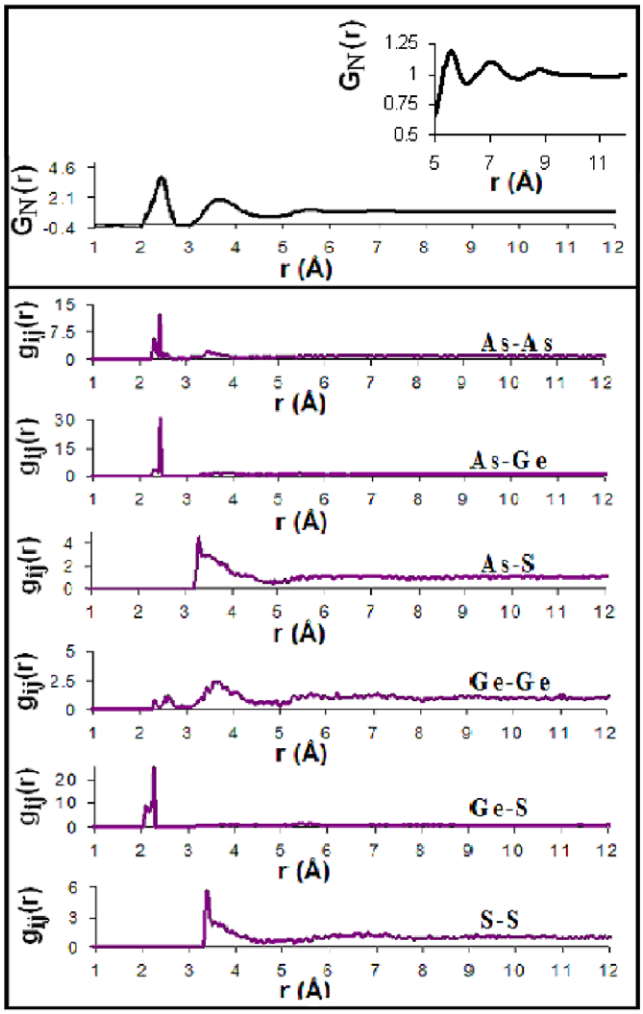

Figure 8. Upper panel: weighted average of the partial pair distribution function $G_N(r)$ for $Ge_{33.3}As_{33.3}S_{33.3}$ glass obtained by neutron diffraction. Inset is a magnified view of $G_N(r)$ at $r \geqslant 5$ Å. Lower panel: partial pair distribution functions $g_{ij}(r)$ for $Ge_{33.3}As_{33.3}S_{33.3}$ glass (case I) obtained from RMC simulations.

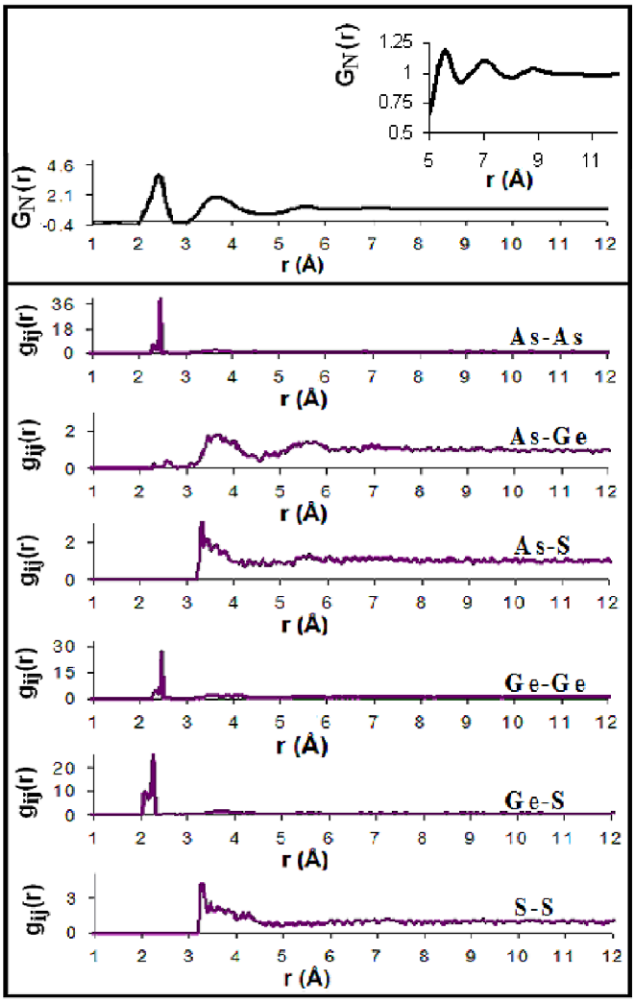

Figure 9. Upper panel: weighted average of the partial pair distribution function $G_N(r)$ for $Ge_{33.3}As_{33.3}S_{33.3}$ glass obtained by neutron diffraction. Inset is a magnified view of $G_N(r)$ at $r \geqslant 5$ Å. Lower panel: partial pair distribution functions $g_{ij}(r)$ for $Ge_{33.3}As_{33.3}S_{33.3}$ glass (case II) obtained from RMC simulations.

decreasing trend in the position of neutron and x-ray FSDP to lower Q values with increasing metal content thus indicates that the length scale of intermediate-range order in the form of metal–metal correlations increases in the system. The RMC generated partial structure factors of the $Ge_xAs_xS_{100-2x}$ glass with $x = 18.2$ (figure 2) clearly show that all of the metal–metal (i.e. As–As, Ge–Ge and As–Ge) correlation structure factors do indeed have intense peaks at $\sim$1.1 Å^{-1} exhibiting a strong contribution to FSDP and therefore to the intermediate-range order at a length scale of $\sim$5.7 Å. On the other hand, the S–S and metal–S structure factors have minor or negligible contribution to the FSDP intensity. The RMC generated atomic configuration for this glass shows the formation of a homogeneously mixed corner-shared network of GeS_4 tetrahedra and AsS_3 pyramids (figure 1(a)). In contrast with this glass only the Ge–Ge and As–As partial structure factors contribute significantly to the FSDP of the $Ge_{25}As_{25}S_{50}$ glass, with a minor contribution from the As–Ge partial (figure 3). This result implies the formation of As-rich regions that are spatially separated from Ge-rich regions in the glass structure. The RMC generated atomic configuration for this glass shows nanoscale clusters of the GeS_2 network and homopolar As–As bonded regions (figure 1(b)). Such nanoscale clustering is consistent with the nearest-neighbor coordination environments of the metal atoms, as determined in a previous Ge and As K-edge EXAFS spectroscopic study that indicated the presence of GeS_4 tetrahedra and $AsAs_3$ pyramids in this glass (table 1). The spatial correlation lengths of the clusters of GeS_2 network and As–As homopolar bonded regions in $Ge_{25}As_{25}S_{50}$ glass, as shown in figure 1(b), is on the order of $\sim$20 Å, which is consistent with the experimentally determined coherence length of $\sim$24 Å [25, 26]. Moreover, such intermediate-range order that leads to Ge- and As-rich regions in the glass structure is also expected to give rise to significantly large density and composition fluctuations. Such a hypothesis is again consistent with the experimentally observed high SANS intensity for this glass. In fact, a comparison of the partial structure factors for all compositions show that the small angle scattering intensity dramatically

increases at $x = 25$ (figures 2–5). Figure 3 clearly indicates that these density fluctuations originate from the long-range metal–metal and S–S correlations, and that the structure of the glass with $x = 25$ is the most heterogeneous on a nanometer length scale.

As mentioned earlier, for $Ge_{33.3}As_{33.3}S_{33.3}$ glass, the relative degree of chemical order in metal–metal bonding involving Ge and As atoms could not be differentiated by combined neutron and x-ray diffraction [25, 26]. Therefore, the nature of intermediate-range order is also not clear for this composition. In order to visualize the structure of this glass, two sets of RMC simulations were performed to illustrate limiting possibilities (table 1). Case I assumed that Ge atoms prefer to bond to As atoms only, while case II assumed Ge atoms are bonded to Ge atoms and As atoms prefer to bond As atoms only. The corresponding experimental and RMC generated structure factors, together with the partial structure factors, are shown in figures 4 and 5, respectively. RMC generated total structure factors for both cases agree with the experimental ones at the same level, therefore, one can not conclusively argue that one structure is more likely than the other on the basis of total structure factors alone. The partial structure factors for case I and case II display the characteristics of the bonding constraints applied in the system. For case I, As–Ge and As–As partial structure factors display peaks at $\sim$1.0 $Å^{-1}$, thus contributing to the FSDP (figure 4). On the other hand As–As and Ge–Ge correlations are the main contributors to FSDP for case II (figure 5). The RMC configuration for case I displays (figure 1(c)) a more homogeneous distribution of metal atoms when compared to that for case II (figure 1(d)), as in the former case Ge atoms were forced to bond to As atoms. For case I, the small angle scattering signal in the metal–metal partials is observed to notably decrease for $Ge_{33.3}As_{33.3}S_{33.3}$ glass, indicating that its structure is significantly more homogeneous on a nanometer length scale compared to that of the $Ge_{25}As_{25}S_{50}$ glass (figures 3 and 4). On the other hand, for case II, all like metal atoms are forced to be bonded to each other i.e. only homopolar As–As and Ge–Ge bonds were allowed, which resulted in an expected As-clustering (figure 1(d)). In fact the topological continuity of As-rich and Ge-rich regions in this glass is found to extend to long length scales of $\sim$23 Å, similar to the As-rich regions in the $Ge_{25}As_{25}S_{50}$ configuration (figure 1(b)). However, experimentally the coherence length of intermediate-range order ($2\pi/\Delta Q_{FSDP}$) as well as the SANS intensity for the $Ge_{33.3}As_{33.3}S_{33.3}$ glass are significantly smaller than those characteristics for the $Ge_{25}As_{25}S_{50}$ glass [25, 26]. These results indicate a more homogeneous spatial distribution of metal atoms in the $Ge_{33.3}As_{33.3}S_{33.3}$ glass compared to that in the $Ge_{25}As_{25}S_{50}$ glass. Hence, the structural scenario represented by case I seems to be more consistent with the experimental results than case II.

5. Summary

RMC simulations of the high energy x-ray and neutron diffraction data have been used to obtain three-dimensional atomic configurations, partial structure factors and partial pair distribution functions for a series of $Ge_xAs_xS_{100-2x}$ glasses with Ge (or As) contents of 18.2, 25, and 33.3%. RMC results suggest that the structure of the stoichiometric $Ge_{18.2}As_{18.2}S_{63.6}$ glass consists of a corner-shared network of homogeneously mixed GeS_4 tetrahedra and AsS_3 pyramids. The corresponding intermediate-range order is associated with the metal–metal correlations in this mixed GeS_2–As_2S_3 network that gives rise to the FSDP. The nanometer-scale coherence length of this order is controlled by the chemical and topological order of the network. An increase in S-deficiency ($x = 25$) results in the formation of heteropolar bonded GeS_2 regions and homopolar bonded As-rich clusters with correlation length on the order of 20 Å in the $Ge_{25}As_{25}S_{50}$ glass. The heterogeneous nature of the structure of this glass, resulting from the coexistence of As-rich regions and GeS_2 network, can be linked to the experimentally observed maxima at or near this composition in the FSDP intensity, coherence length of intermediate-range order and SANS intensity as a function of metal content. Moreover, the correlation length of the GeS_2 and As-rich clusters in this glass corresponds well with the coherence length of intermediate-range order derived from the width of the FSDP. For the most S-deficient $Ge_{33.3}As_{33.3}S_{33.3}$ glass, the topological continuity of GeS_2 and As-rich clusters is disrupted and a relatively more homogeneous Ge–As bonded network is formed as Ge atoms participate in Ge–As type metal–metal bonding.

Acknowledgments

This work was supported by the National Science Foundation Grant DMR 0906070. The work at Argonne National Laboratory was supported by the US Department of Energy, Office of Science, Office of Basic Energy Sciences, under Contract No. DE-AC02-06CH11357.

References

[1] Zakery A and Elliott S R 2003 *J. Non-Cryst. Solids* **330** 1
[2] Shimakawa K, Kolobov A V and Elliott S R 1995 *Adv. Phys.* **44** 475
[3] Georgiev D G, Mitkova M, Boolchand P, Brunklaus G, Eckert H and Micoulaut M 2001 *Phys. Rev.* B **64** 134204
[4] Lowe A J, Elliott S R and Greaves G N 1986 *Phil. Mag.* B **54** 483
[5] Zhou W, Paesler M A and Sayers D E 1991 *Phys. Rev.* B **43** 2315
[6] Zhou W, Paesler M A and Sayers D E 1992 *Phys. Rev.* B **46** 3817
[7] Armand P, Ibanez A, Dexpert H and Philippot E 1992 *J. Non-Cryst. Solids* **139** 137
[8] Eckert H 1994 *NMR: Basic Principles and Prog.* **33** 125
[9] Greaves G N and Sen S 2007 *Adv. Phys.* **56** 1
[10] King W A, Clare A G, LaCourse W C, Volin K, Wright A C and Wanless A J 1997 *Phys. Chem. Glasses* **38** 269
[11] Jackson K, Briley A, Grossman S, Porezag D V and Pederson M R 1999 *Phys. Rev.* B **60** R14985
[12] Petri I, Salmon P S and Fischer H E 2000 *Phys. Rev. Lett.* **84** 2413
[13] Bureau B, Troles J, Le Floch M, Guenot P, Smektala F and Lucas J 2003 *J. Non-Cryst. Solids* **319** 145
[14] Bureau B, Troles J, Le Floch M, Smektala F and Lucas J 2003 *J. Non-Cryst. Solids* **326/327** 58

[15] Bychkov E, Benmore C J and Price D L 2005 *Phys. Rev.* B **72** 172107
[16] Sen S, Ponader C W and Aitken B G 2001 *J. Non-Cryst. Solids* **293–295** 204
[17] Sen S, Ponader C W and Aitken B G 2001 *Phys. Rev.* B **64** 104202
[18] Sen S and Aitken B G 2002 *Phys. Rev.* B **66** 134204
[19] Aitken B G and Ponader C W 2000 *J. Non-Cryst. Solids* **274** 124
[20] Lippens P E, Jumas J C, Olivier-Fourcade J and Aldon L 2000 *J. Non-Cryst. Solids* **271** 119
[21] Mitsa V, Babinets Y, Gvardionov Y and Yermolovich I 1991 *J. Non-Cryst. Solids* **137/138** 959
[22] Boulmetis Y C, Perakis A, Raptis C, Arsova D, Vateva E, Nesheva D and Skordeva E 2004 *J. Non-Cryst. Solids* **347** 187
[23] Mamedov S, Georgiev D G, Qu T and Boolchand P 2003 *J. Phys.: Condens. Matter* **15** S2397
[24] Neov S, Gerasimova I, Skordeva E, Arsova D, Pamukchieva V, Mikula P, Lukas P and Sonntag R 1999 *J. Mater. Sci.* **34** 3669
[25] Soyer Uzun S, Sen S, Benmore C J and Aitken B G 2008 *J. Phys. Chem.* C **112** 7263
[26] Soyer Uzun S, Sen S, Benmore C J and Aitken B G 2008 *J. Phys.: Condens. Matter* **20** 335105
[27] Soyer-Uzun S, Sen S and Aitken B G 2009 *J. Phys. Chem.* C **113** 6231
[28] McGreevy R L and Pusztai L 1988 *Mol. Simul.* **1** 359
[29] McGreevy R L 2001 *J. Phys.: Condens. Matter* **13** R877
[30] Jóvári P, Kaban I, Steiner J, Beuneu B, Schöps A and Webb M A 2008 *Phys. Rev.* B **77** 035202
[31] Murakami Y, Usuki T, Kohara S, Amo Y and Kameda Y 2007 *J. Non-Cryst. Solids* **353** 2035
[32] Kaban I, Jóvári P, Hoyer W and Welter E 2007 *J. Non-Cryst. Solids* **353** 2474
[33] Kaban I, Hoyer W, Petkova T, Petkov P, Beuneu B, Schöps A and Webb M A 2007 *J. Ovonic Res.* **3** 67
[34] Murakami Y, Usuki T, Sakurai M and Kohara S 2007 *Mater. Sci. Eng.* A **449** 544
[35] Kaban I, Jóvári P, Hoyer W and Welter E 2007 *J. Non-Cryst. Solids* **353** 2474
[36] Kaban I, Gruner S, Jóvári P, Kehr M, Hoyer W, Delaplane R G and Popescu M 2007 *J. Phys.: Condens. Matter* **19** 335210
[37] Jóvári P, Kaban I, Hoyer W, Delaplane R G and Wannberg A 2005 *J. Phys.: Condens. Matter* **17** 1529
[38] Zotov N, Bellido F, Dominguez M, Hannon A C and Sonntag R 2006 *Physica* B **276** 463
[39] Zotov N, Jimenez-Garay R, Bellido F, Dominguez M, Hannon A C and Sonntag R 1997 *Physica* B **234** 424
[40] Ellison A J G, Crawford R K, Montague D G, Volin K J and Price D L 1993 *J. Neutron Res.* **1** 61
[41] Arai M, Johnson R W, Price D L, Susman S, Gay M and Enderby J E 1986 *J. Non-Cryst. Solids* **83** 80
[42] Fuoss P H, Eisenbergen P, Warburton W K and Bienenstock A 1981 *Phys. Rev. Lett.* **46** 1537
Barnes A C, Hamilton M A, Buchanan P and Saboungi M-L 1999 *J. Non-Cryst. Solids* **250–252** 393